FORTY-FOURTH ANNUAL SYMPOSIUM ON FREQUENCY CONTROL

INTERFERENCE FRINGES FROM SINGLE-CAVITY EXCITATION OF AN ATOMIC BEAM*

A. DeMarchi,
University of Ancona, Ancona, Italy
and
R. E. Drullinger and J. H. Shirley
Time and Frequency Division
National Institute of Standards and Technology
325 Broadway
Boulder, Colorado 80303

Abstract

A cyclindrical cavity operated in the TE_{013} mode was used for excitation of the hyperfine transition in an optically pumped cesium beam spectrometer. In the configuration we used the atoms see the rf H-field reverse its direction twice. The observed lineshapes show an interference structure similar to Ramsey interference. Theoretically derived lineshapes are in good agreement with the observations. A comparison is made between these lineshapes and corresponding Ramsey lineshapes. The effects of phase variations within the cavity are also discussed briefly.

Introduction

A prototype atomic beam device was set up to test optical pumping as a means of state preparation and detection. Since the magnetic field in this device is longitudinal, a suitable Ramsey-style microwave excitation structure was not readily available. Instead, a simple cylindrical cavity was substituted. This cavity was operated in the TE_{013} mode with the atomic beam passing along the cylindrical axis. The microwave magnetic field amplitude seen by the atoms then has the form of three half periods of a sine wave (see Fig. 1). We expected this form of excitation would exhibit line narrowing similar to that achieved with Ramsey excitation.

Experiment

The prototype beam tube was made as follows. The vacuum chamber was assembled from commercial vacuum components and pumped with a turbo molecular pump. The cesium oven was a piece of 3/8 inch copper tube with a 3 mm graphite aperture. This type of oven does not last long because of the absorption of cesium by graphite, but it is simple to make and delivers a fairly well collimated beam. The laser beams enter and exit the chamber through near normal incidence, high quality anti-reflection coated windows epoxied to the tube. The fluorescence collection optics are identical to those developed for NIST-7 [1]. The C-field coil is wound on an aluminum cylinder with a diameter of about 20 cm. There is a single layer of magnetic shielding with no end caps. The separation of the optical pumping region from the detection region is 25 cm.

The cavity and its mode pattern are shown schematically in Fig. 1. The cavity is made of 2 inch copper plumbing pipe with brass end plugs. The latter have a 5 mm axial hole for the atomic beam passage and a $\lambda/4$ mode filter to discriminate against the degenerate TM and lower modes. The cavity is fed in the center by a small loop in the end of the 0.087 inch coaxial feed line. There is no provision for coupling adjustment. The

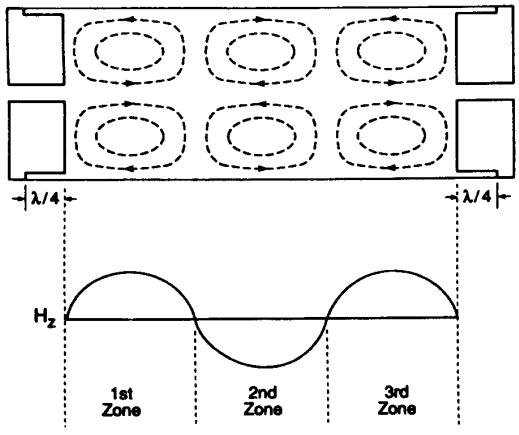

Figure 1. Schematic of TE_{013} mode showing longitudinal magnetic field amplitude in the three excitation zones.

*Contribution of the U.S. Government, not subject to copyright.

resonant frequency was tuned by adjusting the position of the end plugs before they were fixed in place. The final tuning is done by temperature adjustment. The cavity has a loaded Q of about 20 000.

The experiments were done with a single diode laser narrowed by optical feed-back [2] and locked to a saturated absorption feature in a separate cesium cell. A second optical frequency was synthesized from the laser by an acousto-optic modulator. This allowed us to pump on the F = 4 →F'= 4 transition and detect on the F = 4 → F'= 5 cycling transition.

Representative experimental lineshapes for the clock resonance, (F = 3, m = 0 to F = 4, m = 0), are shown in Figs. 2a and 3a together with theoretical lineshapes Figs. 2b and 3b for the same conditions.

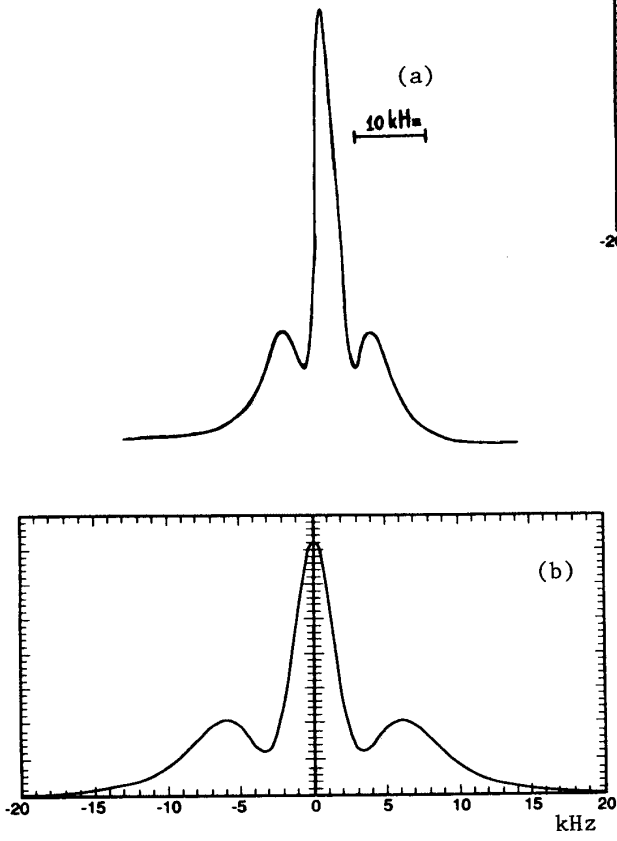

Figure 2. Experimental(a) and theoretical(b) lineshapes obtained at optimum power.

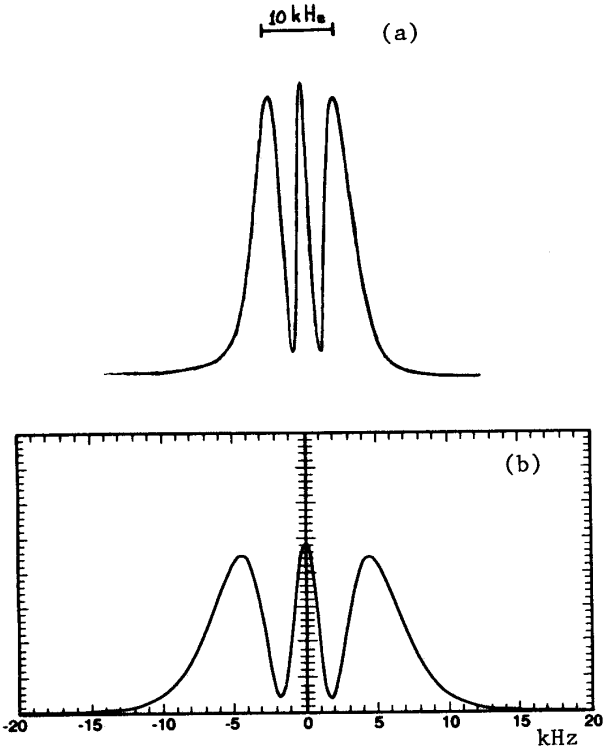

Figure 3. Experimental(a) and theoretical(b) lineshapes obtained at 6 dB below optimum power.

Theory

In the notation of Ramsey [3, Chap. V.3], the evolution of the probability amplitudes of the two hyperfine states is given by the time-dependent Schrodinger equation

$$i(d/dt)C_p(t) = bg(t)e^{i\omega t}C_q(t),$$
$$i(d/dt)C_q(t) = bg(t)e^{-i\omega t}C_p(t) + \omega_o C_q(t), \quad (1)$$

with the initial conditions $C_p(0) = 1$ and $C_q(0) = 0$. We have chosen the energy of the initial state p to be zero. The rotating field approximation has been made. The Rabi frequency 2b is proportional to the microwave magnetic field amplitude, ω is the microwave angular frequency, and ω_0 is the atomic resonance frequency. The function g(t) represents the time dependence of the microwave field amplitude. For the TE_{013} mode g(t) is shown in Fig. 1

and is given by $(\pi/2)\sin(\pi t/\tau)$, where τ is the transit time through one of the three zones, and g is normalized so that $\int_0^\tau g(t)dt = \tau$.

Weak excitation

The theory is most easily developed and understood in the limit of weak excitation. To first order in b, C_p remains equal to 1. The probability amplitude for excitation after an atom has traversed n zones is then

$$C_q = -ibe^{-i\omega_o\tau}G_n(\lambda) \qquad (2)$$

where

$$G_n(\lambda) = \int_0^{n\tau} g(t)e^{i\lambda t}dt = -\frac{\pi^2}{2}\tau\frac{(1-e^{in\lambda\tau}cosn\pi)}{(\lambda^2\tau^2-\pi^2)} \qquad (3)$$

and $\lambda = \omega_0-\omega$ is the detuning from resonance of the microwave field. G_n is well-behaved at $\lambda\tau = \pm\pi$ since both numerator and denominator vanish together for integer n. If we consider the function g(t) to be zero outside the range $0<t<n\tau$, then the integration limits in (3) can be extended to plus and minus infinity and $G_n(\lambda)$ becomes the Fourier transform of g(t). The transition probability becomes

$$P_n(\lambda) = b^2|G_n|^2 = \pi^4b^2\tau^2\frac{\cos^2(n\lambda\tau/2)}{(\lambda^2\tau^2-\pi^2)^2} \qquad (4)$$

for n odd. For n even, replace $\cos(n\lambda\tau/2)$ by $\sin(n\lambda\tau/2)$. The result (4) is shown in Fig. 4 for n=3. With the aid of some trigonometric identities we can factor the transition probability for one zone of excitation from (4):

$$P_n = |F_n|^2P_1. \qquad (5)$$

For n = 3 the remaining factor,

$$F_3 = 2\cos\lambda\tau-1 = e^{i\lambda\tau}-1+e^{-i\lambda\tau}, \qquad (6)$$

is the sum of three exponentials. These exponentials relate the transition amplitude in the second and third zones to that in the first zone by phases that correspond to the difference in phase evolution between the field and the state q. These phases interfere to either destroy or enhance the basic probability P_1. Hence, we refer to F_3 as the interference factor. For $\lambda\tau = \pi$, $F_3 = -3$ and P_3 is enhanced nine times over P_1. This enhancement is shown by the strong side peaks in Fig. 4. The interference factor also narrows the central peak and introduces additional zeros.

Note that if no excitation took place in the second zone, we would have a form of Ramsey excitation with the drift time $T=\tau$. The second term in (6) would then be missing and (5) would reduce to

$$P_R = (2\cos\lambda\tau)^2P_1, \qquad (7)$$

the usual expression for weak two-zone Ramsey excitation [3, Chap. V.4]. This lineshape, also shown in Fig. 4, has a central peak 1.4 times broader than the central peak for three zone excitation. It also has prominent side peaks, but they are not enhanced above the central peak.

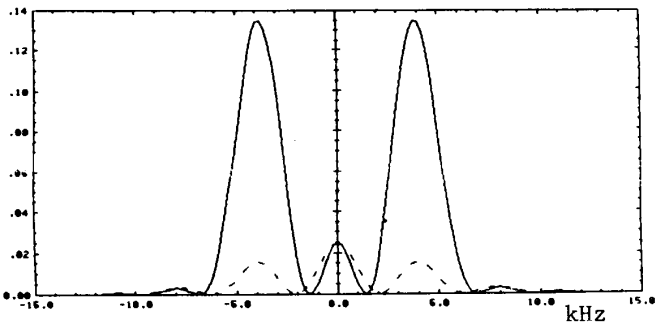

Figure 4. Comparison of lineshapes from three-zone excitation (solid line) with Ramsey excitation (dashed line) at low power with single velocity atoms.

The results (4) and (5) also apply to values of n larger than 3 corresponding to excitation by a TE_{01n} mode. The interference factor F_n becomes a polynomial in $\cos\lambda\tau$ related to the Tschebyscheff polynomials. The lineshape has very strong, narrow side peaks for single-velocity atoms. The central peak has a width $\Delta\nu_n = k_n/2n\tau$ where $k_1 = 2.38$, $k_3 = 1.04$, and k_n approaches unity for n large. A corresponding Ramsey excitation would include excitation by only the first and last zones with a drift time between excitation zones $T = (n-2)\tau$. For such a Ramsey excitation

(7) holds with $\lambda\tau$ replaced by $(n-1)\lambda\tau/2$ in the argument of the cosine. The central peak has a width $\Delta\nu_n = q_n/2(n-1)\tau$ where $q_3 = .98$ and q_n approaches unity for n larger. Hence for n large the multi-zone excitation and corresponding Ramsey excitation yield lineshapes with similar widths.

Strong excitation

If $\psi(t)$ represents the state vector whose components are $C_p(t)$ and $C_q(t)$, then the time evolution of $\psi(t)$ can be expressed by a 2 x 2 evolution matrix $U(t,t_0)$ such that

$$\psi(t) = U(t,t_0)\ \psi(t_0). \qquad (8)$$

For three-zone excitation the evolution can be broken down into the product of evolutions across each zone:

$$\psi(3\tau) = U(3\tau,2\tau)\ U(2\tau,\tau)\ U(\tau,0)\ \psi(0). \qquad (9)$$

In terms of the solution of (1) at $t = \tau$ we have the evolution matrix

$$U(\tau,0) = \begin{pmatrix} C_p(\tau) & -C_q(\tau)^* e^{-i\omega_0\tau} \\ C_q(\tau) & C_p(\tau)^* e^{-i\omega_0\tau} \end{pmatrix}. \qquad (10)$$

$U(2\tau,\tau)$ and $U(3\tau,2\tau)$ are the same as $U(\tau,0)$ except that $C_q(\tau)$ is replaced by $-C_q(\tau)e^{-i\omega\tau}$ and $C_q(\tau)e^{2i\omega\tau}$ respectively. Thus, knowing the solution of (1) for the first excitation zone allows us to easily find the solution for several zones by matrix multiplication. The results for the transition probability are

$$P_1 = |C_q(\tau)|^2 \quad \text{for one zone,}$$

$$P_2 = 4y^2 P_1 \quad \text{for two zones,}$$

$$P_3 = (1-4y^2)^2 P_1 \quad \text{for three zones,} \qquad (11)$$

where $y = \mathrm{Im}[C_p(\tau)\exp(i\lambda\tau/2)]$.

The one-zone transition probability P_1 is again a factor in the multi-zone transition probability. In the weak excitation limit $C_p(\tau)$ is unity so that $y = \sin(\lambda\tau/2)$ in agreement with (6). For stronger excitation $C_p(\tau)$ decreases, making the side peaks less prominent.

For the actual sine-wave form of g(t) the Schrodinger equation (1) was integrated numerically across one zone to find $\psi(\tau)$. The transition probability for 1, 2, and 3 zones was then found from the relations (11). A sample result is plotted in Fig. 5, for optimum power. Saturation reduces the value of y in (11) allowing the central peak to broaden and reducing the side peaks. Also shown in Fig. 5 is the corresponding Ramsey lineshape for two zones of excitation. The central Ramsey peak is now only 0.6 times as wide as for three zone excitation. Saturation does not affect the interference factor for Ramsey excitation.

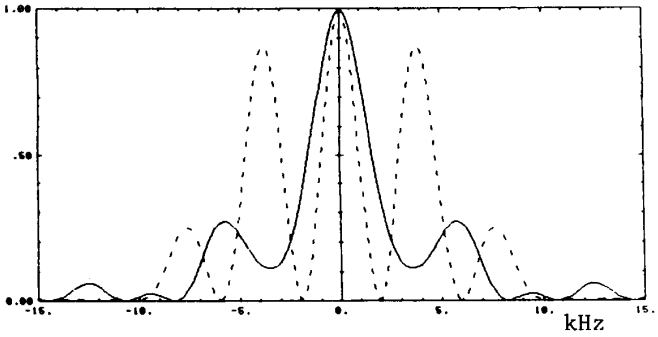

Figure 5. Comparison of lineshapes from three-zone excitation (solid line) with Ramsey excitations (dashed line) at optimum power with single velocity atoms.

Velocity Average

In the experimental situation τ is not fixed, but has a broad distribution of values corresponding to the velocity distribution of atoms in the beam. Since the position of the side lobes, but not the central peak, depends on τ, the side lobes are greatly reduced and broadened by averaging over τ values. A thermal velocity distribution weighted by 1/v for detection by a cycling transition [4] was used to average the numerical results. Figure 2b shows the resulting calculated lineshape for optimum excitation for comparison with the experimental curve in Fig. 2a. At weaker excitation levels, the central peak shrinks and narrows faster than the side lobes as shown in Figs. 3a and 3b. At still lower excitation the central peak becomes only half as high as the side lobes.

Theoretical predictions are in agreement with experimental observations.

Cavity Phase Variations

Spatial phase variations within the cavity can lead to frequency biases, in analogy with the end-to-end phase shift in Ramsey cavities. Only phase variations associated with modes of a symmetry different from the desired one can produce a bias [5]. In our cavity the closest such modes are TE_{012} and TE_{014}. However, since they resonate about 1.1 GHz away from the TE_{013} mode and have very high Q, the resulting frequency bias would be very small even if the cavity feed excited them, which it is not designed to do. An experimental search was made for other modes using probes within the cavity. The only resonances seen in our cavity other than the desired one were those of the TE_{011} and TE_{015} modes, which have a symmetry that will not produce frequency shifts. Furthermore, the degenerate TM_{113} mode and the lower TE_{11n} modes were not observed, indicating that the mode filter works well. In conclusion, we feel that spatial phase variations can be analyzed and shown not to be a problem in this type of cavity.

References

[1] R. E. Drullinger, Jon Shirley, D. J. Glaze, L. W. Hollberg and A. DeMarchi, "Progress Toward an Optically Pumped Cesium Beam Frequency Standard" in Proc. 40th Annual Symposium on Frequency Control, pp. 428-431, 1986.

[2] B. Dahmani, L. Hollberg, and R. Drullinger, "Frequency Stabilization of Semiconductor Lasers by Resonant Optical Feedback", Optics Letters, vol. 12, 876-878, 1987.

[3] N. F. Ramsey, Molecular Beams, Oxford University Press, London, 1956.

[4] G. Avila, E. de Clercq, M. de Labachelerie, and P. Cerez, "Microwave Ramsey Resonances from a Laser Diode Optically Pumped Cesium Beam Resonator," IEEE Trans. Inst. Meas. vol. IM-34, 139-143, 1985.

[5] A. de Marchi, O. Francescangeli, G.P. Bava, "Feasibility of End-to-End Phase Shift Correction from the Outside of Sealed Cesium Beam Tubes," CPEM 1990 (to be published in IEEE Trans. Inst. Meas.).